Thermochimica Acta, 178 (1991) 99–107
Elsevier Science Publishers B.V., Amsterdam

THE SINTERING KINETICS OF REACTION BONDED SILICON NITRIDE BY USING NON-ISOTHERMAL TECHNIQUE

ÇETİN GÜLER

Department of Chemistry, Faculty of Science, University of Ege, Izmir (Turkey)

(Received 19 June 1990)

ABSTRACT

The sintering kinetics of reaction bonded silicon nitride (RBSN) with 4.3% of Y_2O_3 and 1.4% of Al_2O_3 were investigated under non-isothermal conditions at various constant heating rates. The activation energy was found to be ≈ 670 kJ mol^{-1}.

The density of RBSN increased from 2.55 g cm^{-3} to 3.09 g cm^{-3} and also the room temperature strength increased from 224 to 424 MN m^{-2} with decreasing heating rate.

INTRODUCTION

Sintered silicon nitride ceramics are used as structural materials, e.g., in making components for gas turbine engines and turbocharger reactors, and in various diesel engine components, because they have high mechanical and chemical strength, good thermal shock resistance and oxidation–corrosion resistance at high temperature [1–5]. The density of Si_3N_4 must be higher than 95% of theoretical if it is to be used as an engineering material, and the shrinkage must be within certain limits to allow the control of complex shapes.

Silicon nitride components can be prepared by sintering very fine powders to give high densities. However, the densities of these compacts are usually limited to about 55% and, on sintering, such bodies would undergo a linear shrinkage of about 17%. Shrinkage of that magnitude would make close dimensional control of complex shapes very difficult to achieve [6].

Silicon nitride, furthermore, can be prepared by using hot-pressing (HPSN) and cold-forming (SSN) methods [6]. In the hot-pressing method, certain sintering aids are added to the silicon nitride, which is then densified under pressure at high temperatures. The strength of hot-pressed silicone nitride is very high, but only very simple shapes can be produced directly; more complex components require expensive grinding with diamond-impregnated wheels. In the cold-forming method, sintering aids are used in large quantities.

0040-6031/90/$03.50

Silicon nitride can also be formed by reacting compacted silicon powders with nitrogen to form reaction-bonded silicon nitride (RBSN) bodies [7]. These components can be formed close to the required shape, with a high degree of dimensional control, because no shrinkage occurs during reaction with the inclusion of appropriate sintering aids, such as MgO, Y_2O_3, Al_2O_3 and $BeSiN_2$ [8]. Densification of RBSN can be achieved under appropriate sintering conditions.

An important factor in the sintering is the thermal decomposition of Si_3N_4. This is influenced by the silicon nitride material, the SiO_2 on the nitride particles and the presence of oxide sintering aids; the main gaseous decomposition products are $N_2(g)$ and SiO(g) in the graphite resistance furnace and the graphite container [9]. Decomposition may be suppressed by increasing the absolute pressure of nitrogen and by embedding the specimens in a protective powder bed [10].

In this study, the sintering kinetics of RBSN with increasing temperature and at various heating rates has been investigated. The first theoretical and practical studies concerning non-isothermal kinetics were published in the 1950s and have since been improved on [11–15].

The change of linear shrinkage with time is described by the following equation [16],

$$\frac{\Delta L}{L_0} \propto \frac{D}{T} t^m \tag{1}$$

A special case arises if the temperature variation is given by the equation [17]

$$\frac{1}{T} = a - bt \tag{2}$$

where $a = 1/T_0$, $b = 1/T_0^2$ and β is the heating rate (T_0 can be obtained by using a graph of T vs. time).

Substitution in eqn. (1) and, if the temperature rises at a constant rate (β), differentiation lead to

$$\frac{1}{m}\left(\frac{\Delta L}{L_0}\right)^{(1-m)/m} \times \mathrm{d}\left(\frac{\Delta L}{L_0}\right) = -K\frac{D}{bT}\mathrm{d}\left(\frac{1}{T}\right) \tag{3}$$

After substitution of $D = D_0 \exp(-E/RT)$ and by integration of eqn. (3) we get

$$\left(\frac{\Delta L}{L_0}\right)^{1/m} = \frac{K'}{\beta} \exp(-E/RT) \tag{4}$$

where K' is the sum of different physical constants.

Equation (4) can be written in logarithmic form

$$\ln\left(\frac{\Delta L}{L_0}\right) = m \ln\frac{K'}{\beta} - mE/RT \tag{5}$$

Assuming the extents of linear shrinkage to be constant for different constant heating rates, eqn. (4) can be written as

$$\ln \beta = \ln K'' - E/RT \tag{6}$$

where E is the activation energy of the sintering process.

The slope of a plot of $\ln(\Delta L/L_0)$ vs. $1/T$ is $m_1(= -mE/R)$ and that of a plot of $\ln \beta$ vs. $1/T$ is $m_2(= -E/R)$. The exponents m and E can be determined from m_1 and m_2.

EXPERIMENTAL

The sintering was carried out in a graphite resistance furnace (Astro Industries). A high temperature dilatometer was attached at each end of the furnace for measuring the shrinkage of the specimens. The specimens ($4 \times 5 \times 50$ mm^3) were embedded in a protective bed in a graphite container. The temperature was measured with a pyrometer. For temperature control a programmable system was used. The nitrogen gas flow was kept at 4–6 l h^{-1}.

All specimens were rapidly heated up to 1400 °C, then heated at various constant heating rates up to the maximum sintering temperature.

The designations of the specimens and their compositions are given in Table 1.

RESULTS

Firstly, all materials were heated at constant heating rate (20 K min^{-1}) up to sintering temperature (1850 °C) and then held for 1 h at this temperature. The results are shown in Table 2.

The mass of the samples has increased except for material A. This could be due to diffusion of yttrium from the powder bed into the samples.

Sample material A has been used for kinetic studies because it has the greatest density and bending strength.

TABLE 1

Sample	Additive material (%)	
	Y_2O_3	Al_2O_3
A	4.3	1.4
B	5.2	0.6
C	3.0	2.6
D	2.2	4.7

TABLE 2

Sample	Shrinkage (%)	Density (g cm^{-3})	TD [a] (%)	Mass change (%)	Strength (MN m^{-2})
A	6.9	3.12	96.3	−0.2	388
B	4.3	2.96	90.0	+0.1	304
C	5.2	3.12	95.4	−1.2	365
D	5.2	3.10	94.5	+0.7	372

[a] TD = theoretical density.

The shrinkage of material A begins at about 1450 ° C (Fig. 1). The starting point of shrinkage is shifted to higher temperatures by increasing the heating rate, as is the maximum of the shrinkage rate (Fig. 2). Some expansion has been observed in the samples after the initial shrinkage.

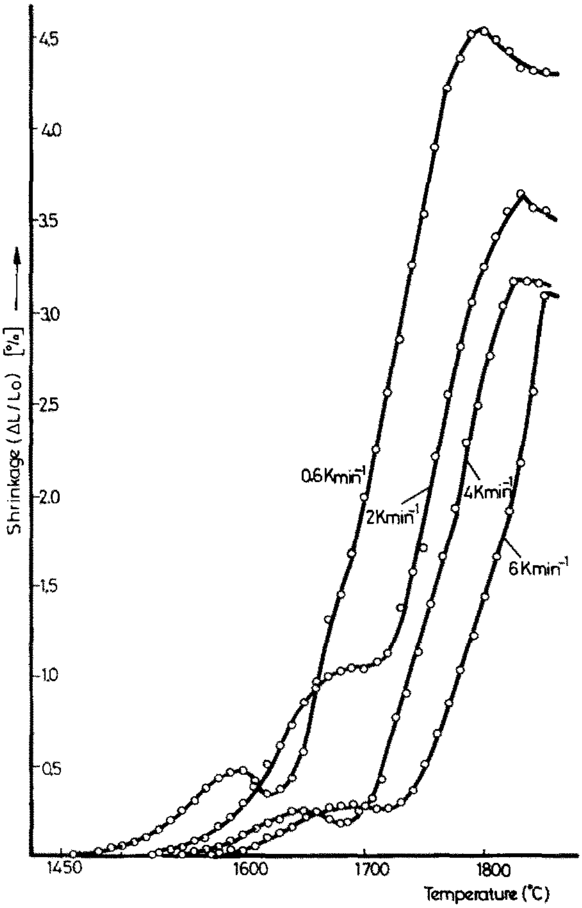

Fig. 1. Linear shrinkage vs. sintering temperature at different heating rates (material A).

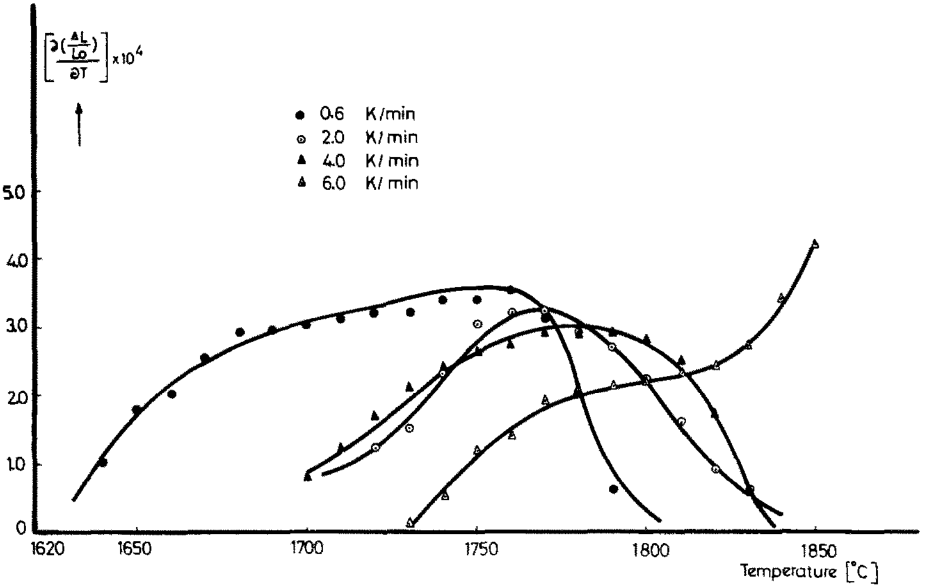

Fig. 2. Dependence of linear shrinkage rate on sintering temperature (material A).

In order to use eqn. (2), the reciprocal temperature plotted against the time must be linear after the T_0 value, as shown in Fig. 3. The logarithms of shrinkages in percent were plotted against the reciprocal of temperature for

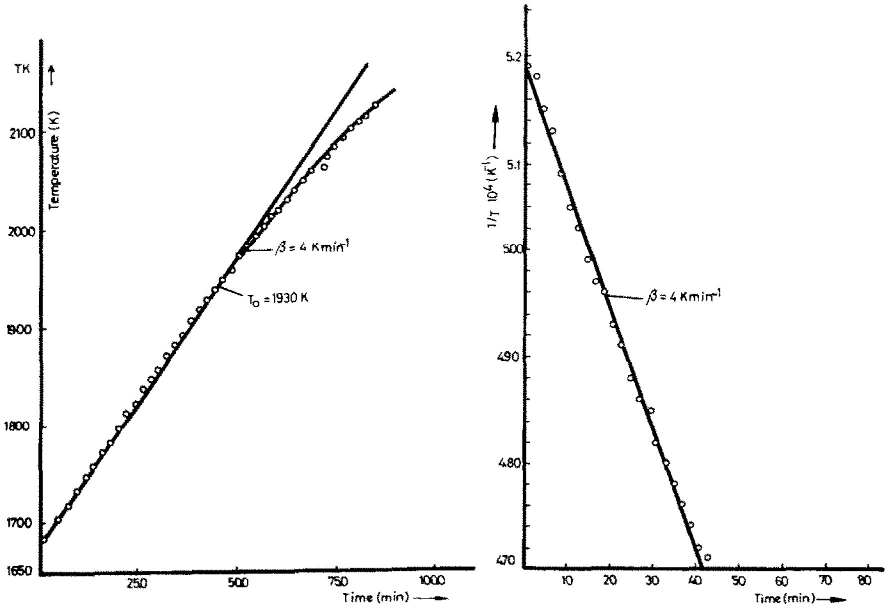

Fig. 3. Temperature and reciprocal temperature vs. time for constant heating rate of 4 K min^{-1}.

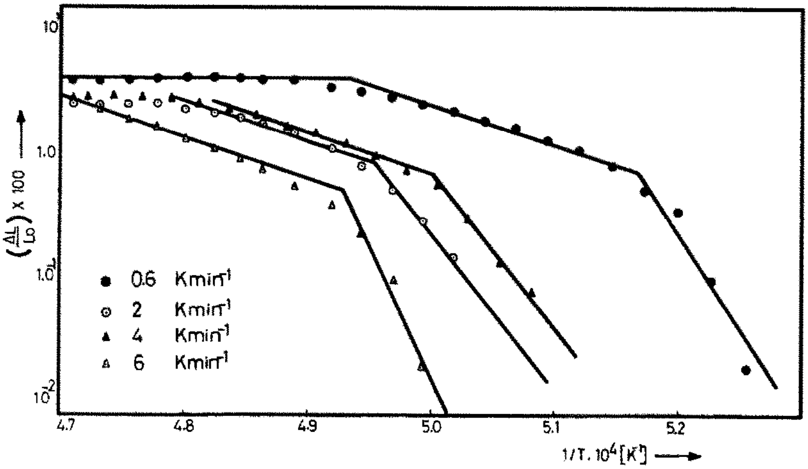

Fig. 4. Log of linear shrinkage vs. reciprocal temperature (material A).

different constant heating rates. Three steps can be distinguished in these curves (Fig. 4). The middle steps of these lines are parallel, and give $m_2 = 78{,}150$.

According to eqn. (6) for the assumed shrinkages, the temperatures have been plotted at which the samples attain the assumed shrinkage at various heating rates (see Fig. 5). The slopes of these lines were determined. The exponent m and the activation energies were calculated for each heating rate, and are given in Table 3.

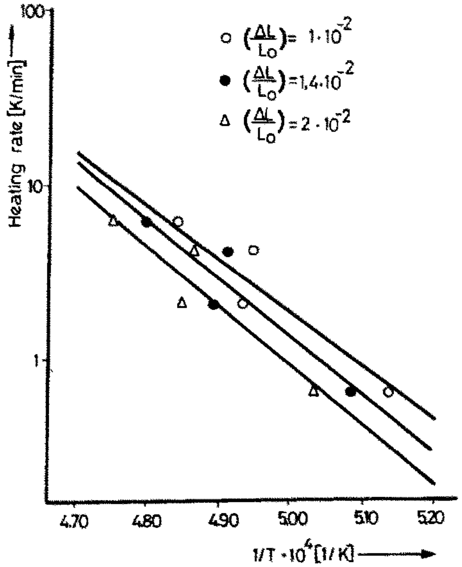

Fig. 5. Graph of ln β vs. $1/T$ for various values of $\Delta L/L_0$ (material A).

TABLE 3

Heating rate, β (K min^{-1})	Slope, m_1	Exponent m	Activation energy, E (kJ mol^{-1})
0.6	−68700	0.88	670
2	−82100	1.05	673
4	−80450	1.03	674
6	−81690	1.05	672

The densities reached and the bending strength plotted vs. heating rate are presented in Fig. 6.

Figure 7 shows micrographs of samples in the as-received state and after different post-sintering conditions.

DISCUSSION

In this study, during post-sintering of RBSN containing 4,3% of Y_2O_3 and 1.4% of Al_2O_3 densities of up to 96% of theoretical have been achieved and the bending strength was increased by 96% in comparison with the "green" sample. The pores smaller than 10 μm, have been eliminated, but larger pores are still present.

The shrinkage begins at about 1450 °C. Around that temperature Si–Al–Y–N–O systems have a eutectic [9]. Since some mullite-like compounds and other compounds form at or near this temperature [10], the expansion can be attributed to this formation of new phases.

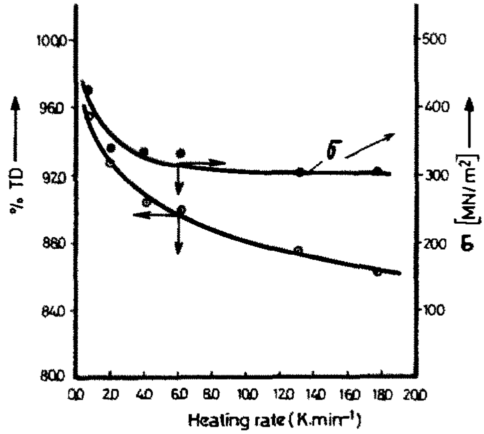

Fig. 6. Density and bending strength vs. heating rate for sintered reaction bonded silicon nitride (SRBSN), (material A).

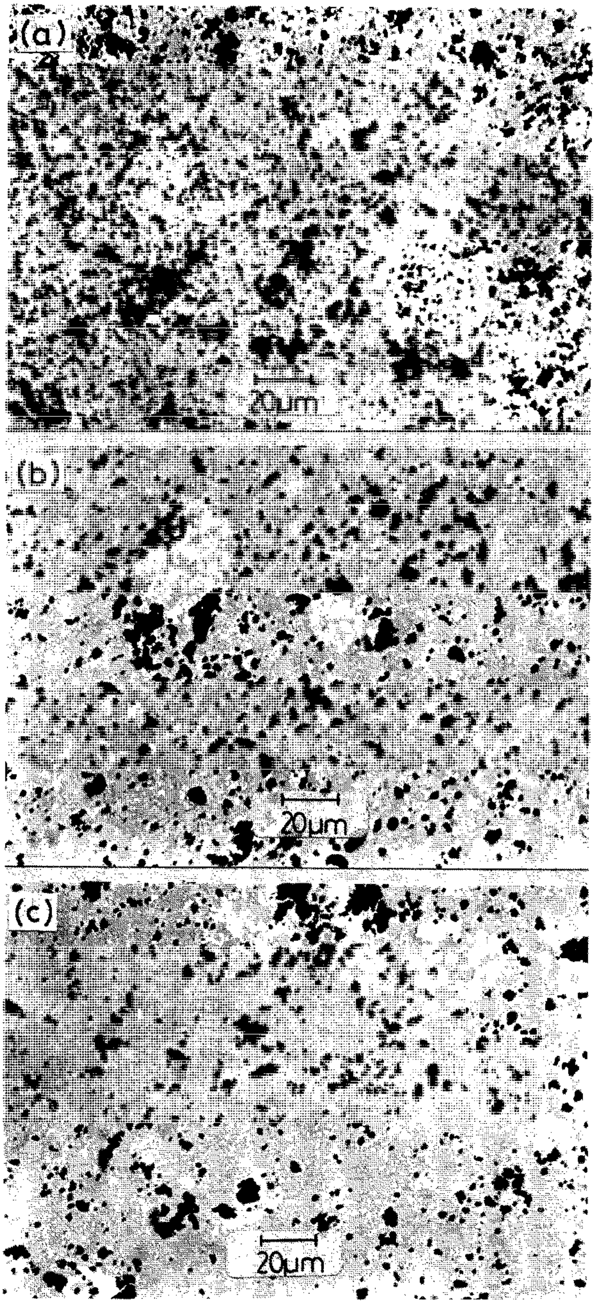

Fig. 7. Microstructure of SRBNS: (a) green sample; (b) sintered at 1850 °C at 6 K min^{-1} heating rate; (c) sintered at 1850 °C at 0.6 K min^{-1} heating rate.

The sintering occurs by a liquid-phase mechanism. In the liquid-phase sintering, densification is considered to occur in three steps [2]: (a) formation of a liquid phase and initial particle arrangement, (b) solution of the solid phase in the liquid followed by precipitation, and (c) the development of a solid framework, which slows the rate of densification. The straight line segments corresponding to the three sintering stages are shown in Fig. 6.

The time exponent of the second step of sintering was found to be between 0.88 and 1.05 for the sintering process of RBSN with 4.3% of Y_2O_3 and 1.4% of Al_2O_3. This value is larger than that for Si_3N_4 powder with Y_2O_3 and Al_2O_3 [11] and half to one-third of that predicted by the Kingery model [3]. This last value is the one expected, but the standard treatment of liquid-phase sintering kinetics does not allow for the phase changes or chemical reactions which occur in the present system. Thus, the solid–liquid reactivity increases [11]. The activation energy for sintering of about 670 kJ mol^{-1} is similar to the activation energy for Si_3N_4 solubility in glass [18].

ACKNOWLEDGEMENTS

This work was performed within a fellowship of the International Seminar Karslruhe at the Institut von des Werkstoffkunde II, University of Karlsruhe in 1983.

The author is indebted to DAAD (Deutscher Akademischer Austauschdienst) for financial support of the research.

REFERENCES

1 J. Mortimer, Engineer, 243 (1976) 56.
2 H.J. Förster and B.E. Lübbing, Automobil Industrie, 25 (1980) 83.
3 J.D. Walton, Jr., Am. Ceram. Soc. Bull., 53 (1974) 255.
4 G. Willmann, Ber. Dtsch. Keram. Ges., 58 (1981) 153.
5 F.W. Clinard, Jr., J. Nucl. Mater., 85/86 (1979) 393.
6 J.A. Mangels and G.J. Tennenhouse, Am. Ceram. Soc. Bull., 59 (1980) 1216.
7 A.J. Moulson, J. Mater. Sci., 14 (1979) 1017.
8 P. Popper, in F.L. Riley (Ed.), Progress in Nitrogen Ceramics. Martinus Nijhoff, The Hague, 1983, p. 187.
9 J.P. Torre and A. Mocellin, in F.L. Riley (Ed.), Nitrogen Ceramics, Leyden, Noordhoff, 1977, p. 63.
10 R.J. Lumby, R.R. Wills and F.R. Horsley, Br. Patent, 1, 448, 732, 1976.
11 P. Duwez and H. Martin, Trans. Metall. Soc. AIME, 185 (1949) 571.
12 T.P. Hoar and J.M. Butler, J. Inst. Met. 7 (1950/51) 351.
13 W.S. Young and I.B. Cutler, J. Am. Ceram. Soc., 53 (1970) 659.
14 D.A. Venkatu and D.L. Johnson, J. Am. Ceram. Soc., 54 (1971) 641.
15 D. Uskovic, J. Pethovic and M.M. Ristic, in G.C. Kuczynski (Ed.), Sintering and Catalysis, Plenum, New York, 1975, p. 315.
16 F. Thümmler and W. Thomma, Metall. Rev., 12 (1967) 69.
17 S.K. Dixit, Thermochim. Acta, 54 (1982) 245.
18 R.L. Tsai and R. Raj, J. Am. Ceram. Soc., 65 (1982) 270.